

1  
2  
3  
4  
5  
6  
7  
8  
9  
10  
11  
12  
13  
14  
15  
16  
17  
18  
19  
20  
21  
22  
23  
24

MISS YI FAN (Orcid ID : 0000-0002-9230-6351)

Article type : Original Paper

### Quantification of Mandibular Sexual Dimorphism during Adolescence

Yi Fan<sup>1,2</sup>, Anthony Penington<sup>2,3</sup>, Nicky Kilpatrick<sup>2,3</sup>, Rita Hardiman<sup>1</sup>, Paul Schneider<sup>1</sup>, John  
Clement<sup>1,2,4</sup>, Peter Claes<sup>2,5,6</sup>, Harold Matthews<sup>2,3</sup>

<sup>1</sup>The University of Melbourne Department of Dentistry, Melbourne, Australia

<sup>2</sup>Murdoch Children's Research Institute, Melbourne, Australia

<sup>3</sup>The University of Melbourne Department of Paediatrics at the Royal Children's Hospital,  
Melbourne, Australia;

<sup>4</sup>Cranfield University, England, UK;

<sup>5</sup>KU Leuven Department of Electrical Engineering, PSI, Leuven, Belgium

<sup>6</sup>Medical Imaging Research Center, Leuven, Belgium

**Corresponding author:** Yi Fan

E-mail: fan2@student.unmelb.edu.au

Address: 50 Flemington Rd, Parkville VIC 3052

Tel: +61 3 9936 6156

This is the author manuscript accepted for publication and has undergone full peer review but has not been through the copyediting, typesetting, pagination and proofreading process, which may lead to differences between this version and the [Version of Record](#). Please cite this article as [doi: 10.1111/JOA.12949](https://doi.org/10.1111/JOA.12949)

This article is protected by copyright. All rights reserved

25

26

27 **Abstract**

28 The present study investigates how sexual dimorphism in the human mandible develops in 3D  
29 during adolescence. A cross-sectional sample of mandibular meshes of 268 males and 386  
30 females, aged between 8.5 and 19.5 years of age, were derived from cone beam computed  
31 tomography and were analyzed using geometric morphometric methods. Growth trajectories of  
32 the mandible in males and females were modeled separately using a recently developed  
33 non-linear kernel regression framework. Growth rate and direction at a dense array of points all  
34 over the mandibular surface were visualized within each group and compared between groups.  
35 We found that mandibular sexual dimorphism already exists at nine years of age, but this is  
36 mostly in size not in shape. The differential growth rate and duration between the sexes during  
37 pubertal growth largely explained the adult sexual dimorphism: growth direction in both males  
38 and females is similar but the male mandible changed more quickly and over a longer period  
39 than the female mandible, where the growth rate peaked and declined earlier. This results in  
40 increasing dimorphism in form which is evident in both size and shape. The development of  
41 dimorphic features, concentrating in the chin and ramus, were further visualized. The dense  
42 morphometric approach provides detailed quantitative assessment of the development of sexual  
43 dimorphism of the mandible in 3D.

44

45 **Keywords:** mandible, sexual dimorphism, ontogeny, geometric morphometrics, CBCT

46

47

48 **Introduction**

49 The mandible is the largest bone of the human face and continuously adapts to functional  
50 demands during growth. Although dynamic mandibular changes from childhood to adulthood  
51 have been documented, how and when each region develops in three dimensions is not fully  
52 understood. Dimorphism of the adult human mandible has been documented in diverse  
53 populations (Hu et al. 2006; Kharoshah et al. 2010; Sharma et al. 2016). However, the  
54 development of sexual dimorphism of the adult mandible has received little attention.

55

56 Traditional anthropometry, using calipers or rulers, can be performed directly on dried mandible  
57 specimens. The morphological change of the mandible is measured and compared between  
58 different individuals at different stages of development (Popa et al. 2009). However, using  
59 anthropometric apparatus, exact measurements of the morphological changes of the bone are  
60 difficult to obtain. When performed on living subjects, the measuring instruments must be  
61 placed on the soft tissues overlying the bony landmarks, reducing the accuracy of measurements  
62 (van der Haven et al. 1997). The bone remodeling processes of deposition and resorption have  
63 been evaluated in histological studies (Enlow & Harris, 1964) but such studies are limited by the  
64 availability of cadavers and do not allow repeated measurement. Radiographic cephalometry has  
65 permitted the study of mandibular growth in living children (Björk 1963; Björk 1968). Although  
66 the mandible has been measured extensively and reported using cephalometrics, three problems  
67 remain: (1) the 2D radiograph is adversely affected by projection distortion and positioning of the  
68 subject, making it hard to standardize the images and compare results between different studies  
69 (Moyers & Bookstein 1979); (2) commonly used 2D lateral cephalometrics emphasize changes in  
70 the sagittal and vertical dimensions, changes in the transverse dimension are missing; (3) the  
71 mandible has always been represented by sparse landmarks. The morphological changes during  
72 growth and development has been oversimplified as incremental changes in linear distances or  
73 angles. Arguably these do not accurately represent the changes in the full 3D structure.

74

75 Clinicians have entered the next phase of diagnostic evaluation and treatment planning using 3D  
76 imaging. Among them, Cone beam computed tomography (CBCT) provides an effective, rapid  
77 scan of the head that depicts undistorted craniofacial structures giving a lower radiation dose  
78 than conventional CT. In recent years, new methodologies using computational approaches for  
79 evaluating craniofacial structures have been developed to augment conventional cephalometry  
80 (Wei et al. 2011; Franchi et al. 2001). Geometric morphometrics – the statistical analysis of shape  
81 and form, abandons traditional linear, angular, or volumetric variables and provides methods of  
82 evaluating the entire 3D structure (Mitteroecker & Gunz, 2009). However, little information is  
83 available in the literature about the morphological changes of the mandible in 3D, especially how  
84 sex differences of the mandible emerge during adolescence. An in-depth understanding of how

85 sexual dimorphism arises during ontogeny is likely to lead to better understanding of the  
86 functional and developmental influences that underpin variation. Further, such understanding  
87 opens up new possibilities for practical applications such as evaluation of craniofacial  
88 abnormalities and determining age and sex of the found remains of juveniles.

89  
90 Using a large cross-sectional database of pre-orthodontic treatment CBCT images, we model the  
91 growth trajectories of human mandibles in males and females separately, using a recently  
92 developed non-linear modelling framework (Matthews et al. 2018). We examine the rate and  
93 direction of change within each group and compare the growth trajectories to examine how  
94 sexual dimorphism in the mandible develops during adolescence.

95

## 96 **Methods**

### 97 **Image data**

98 The CBCT images of untreated adolescent patients were retrospectively sourced from an  
99 orthodontic clinic in Melbourne, Australia, where images had previously been obtained for  
100 clinical indications. Ethics approval for this study was obtained from the University of Melbourne  
101 Human Research Ethics Committee (HREC ID: 1647544.1). The CBCT scans were anonymized  
102 except for information about sex and age. All images were taken using an i-Cat Flx machine  
103 (Imaging Sciences International, PA, USA) with a standardized protocol. While it was not possible  
104 to definitively determine ethnicity, the patient population was predominantly European.  
105 Corresponding facial images were reviewed and patients of non-Caucasian appearance were  
106 excluded, as were patients with defined craniofacial abnormalities. CBCTs were screened for  
107 evidence of previous trauma or multiple missing teeth and detected cases excluded.

108

109 The remaining images were then statistically screened for outliers to remove extreme individuals.  
110 This was achieved by adapting a standard procedure for multivariate outlier detection. A  
111 particular patient was determined to be an outlier and removed from the analysis if its  
112 Mahalanobis distance exceeds a threshold distance corresponding to a p-value of 0.01 (Brereton,  
113 2015). The computation of the Mahalanobis distance used an age appropriate estimate of the

114 covariance calculated separately for each participant. This was defined by a weighted principal  
115 components analysis, retaining PCs that explain 98 percent of the variance (Matthews, 2018). The  
116 participant was excluded from the calculation of the covariance. In total, 268 males and 386  
117 females, ranging from 8.5 to 19.5 years of age were included. The age distribution of the sample  
118 is plotted in Figure 1.

119

#### 120 **Automatic mandible segmentation from CBCT images**

121 The mandible was automatically segmented from each CBCT image of the head using previous  
122 validated approach (Fan et al. 2018). The outer surface of the mandible was tessellated with the  
123 standard marching cubes technique in MATLAB software  
124 (<https://au.mathworks.com/help/matlab/ref/isosurface.html>). Each mandible was then  
125 represented by a surface mesh composed of a dense cloud of points linked to define the surface  
126 of the mandible.

127

#### 128 **Template mapping and mandible registration**

129 Existing spatially-dense morphometric techniques were used to register the mandibles (Claes et  
130 al. 2012a). Essentially, a generic mandibular template, represented by 17,415 quasi-landmarks,  
131 was warped into the shape of each mandible. After template mapping, each quasi-landmark  
132 occupies the same position on a given mandible as on all the other mandibles. In other words,  
133 each quasi-landmark is a single measurement in a specific anatomical location of the mandible,  
134 making spatially dense measurements consistent across all mandibles. The mapping was  
135 conducted with an open source implementation available  
136 at <https://github.com/TheWebMonks/meshmonk>. All the mandibles were made symmetrical by  
137 averaging the original mandible and its own mirror version, so that only the symmetrical  
138 component of shape variation was analyzed. All the mandibles were translated and rotated into a  
139 common frame of reference using Generalized Procrustes Analysis (GPA) with robust Procrustes  
140 superimposition (Claes et al. 2012b). Those quasi-landmarks indicating teeth were cut off so that  
141 only the non-dental component of the mandible was investigated.

142

#### 143 **Modelling the morphological change of the mandible as a function of age**

This article is protected by copyright. All rights reserved

144 To model change in the mandible we follow the basic principle of the non-linear, non-parametric  
145 Nadaraya-Watson kernel regression (Watson 1964; Nadaraya 1965), as adapted for  
146 high-dimensional multivariate shape or form data by Hutton et al. (2003) and Matthews et al.  
147 (2018). The goal is to estimate the expected shape or form of the mandible at each age as well as  
148 the expected rate and direction of change at each point on the mandible. Briefly, for any given  
149 target age, a weighted linear partial least-squares regression (PLSR) of quasi-landmark  
150 co-ordinates onto age was fitted. The weights emphasized those cases closest in age to the target  
151 age and de-emphasized those further away. As these weightings change depending on the target  
152 age, the predicted mandible and predicted the growth rate can change non-linearly. This PLSR  
153 model is used to predict the expected shape or form of the mandible at the target age. The  
154 regression coefficients also provide information about the typical growth direction and rate of  
155 change at each point on the mandible. Specifically, they comprise coefficients on each quasi  
156 landmark co-ordinate, estimating the typical amount of change per year in each direction at each  
157 point. The weights declined from the target age according to a Gaussian function. The standard  
158 deviation of this Gaussian is the only tunable parameter of the model. This was optimized using a  
159 repeated grid-search (Krstajic et al. 2014). We model growth trajectories separately for males and  
160 females but use the same standard deviation for both.

161

162 Specifically, we measured the size of the mandible as the mean distance of each point on the  
163 mandible from its centroid and compared growth trajectories in size of males and females. Total  
164 form changes were visualized along the surface normals of each expected mandible at 9 year of  
165 age and in the vertical, transverse and sagittal dimensions using color maps. The growth direction  
166 and growth rate of the mandibles were compared between males and females.

167

168 We analyze growth rate and direction in terms of form (size and shape together) as this is closest  
169 to the biological reality. For these analyses, mandibles were not scaled to a common size. We also  
170 further investigate sexual dimorphism in shape by scaling each mandible to unit centroid size  
171 during GPA and re-fitting the kernel regression models. This was done because the shape of the  
172 mandible could be useful for sexing fossilized crania.

173

174 **Results**

175 **Mandibular size**

176 Figure 2 demonstrates the change in mandibular size as a function of age. The two lines  
177 represent the expected size of mandibles with the 95% confidence intervals for both males and  
178 females. In general, the size of the mandible was larger in males than in females at all ages  
179 studied. The size difference became greater as the size of the mandible increased more rapidly in  
180 males than in females. The rate of mandibular size change slowed at approximately 14 years in  
181 females but continued to change at a faster rate until it plateaued at 17 years in males.

182

183 **Total form changes**

184 Figure 3 shows the estimated form changes between 9 and 19 years. The mandibular body  
185 became elongated, indicated by the chin projecting anteriorly and the ramus projecting  
186 posteriorly. The condyles elongated predominantly posteriorly and superiorly. The ramus height  
187 increased vertically, and the two sides of the ramus diverged outward to increase inter-ramus  
188 distance. The total change, plotted as colormaps, show the pattern of growth across the  
189 mandible. The morphological changes occur at similar regions but with different magnitude  
190 between males and females. The total amount of change in males was much larger than in  
191 females. For example, color red indicates more than 10 mm expected outward change at the chin  
192 and the condyles in males from 9 years to 19 years, but only approximately half the amount of  
193 change in females over the same period. The overall amount of change was larger in the sagittal  
194 and vertical dimensions than in the transverse dimension.

195

196 **Growth rate and direction in form**

197 The velocity of the annual form changes for males and females, as well as the difference in  
198 growth rate between the sexes, are plotted on the expected mandibles at some selected ages  
199 (Figure 4). The rate of change for males and females averaged over all points on the mandible are  
200 plotted with 95% confidence intervals in Figure 5. In general, the direction of mandibular growth  
201 was similar for both males and females. The growth rate was similar at 9-10 years for both sexes..  
202 Active growth occurred at the condyles and the chin, and, to a lesser degree on the ramus and

203 the mandibular body. The growth rate became slower from age 9 and visually plateaued by 16  
204 years of age in females. Males accelerated from age 9 to 14. The condyles and the chin continued  
205 to change even at 18 years in males.

206

### 207 **Sexual dimorphism in shape**

208 The shape differences between expected mandibles are visualized using colormaps in the first  
209 row in Figure 6. P values at each age were calculated by comparing the observed Procrustes  
210 distance between the male and female expected mandibles to an empirically estimated sampling  
211 distribution. This sampling distribution was estimated by permuting the group labels and refitting  
212 the regression models and calculating the Procrustes distance between mandibles 10,000 times.  
213 Exaggerated mandibles were produced by adding twice the difference between the expected  
214 male and female mandibles onto the expected mandibles at each age. These are plotted in the  
215 second and third rows. Sexual dimorphism in shape is not statistically significant until around age  
216 11 ( $P < 0.05$ ). The exaggerated figures showed that females were characterized by a more obtuse  
217 gonial angle and a narrower chin than in males. These two traits became more distinct from 9 to  
218 19 year of age.

219

### 220 **Discussion**

221 In this study, we use a large sample of human mandibles to model the non-linear growth  
222 trajectories of size, shape and form, and measure sex differences in growth rate and direction  
223 during adolescence in 3D. We find that mandibular sexual dimorphism already exists at nine  
224 years of age, but this is mostly in size. We did not find significant dimorphism in shape at 9 years,  
225 but this could reflect a lack of statistical power. Significant dimorphism was evident by 11 years  
226 and increased through adolescence. Growth direction in both males and females is similar but is  
227 faster, peaks later, and occurs over a longer period in males than in females. This results in  
228 increasing dimorphism in form which is evident in both size and shape.

229

230 The growth of the craniofacial complex is governed by a combination of predetermined genetic  
231 blueprint and epigenetic factors such as mechanical forces and function (Carlson 2005). The  
232 mandible has movable articulations with the basicranium and continuously adapts to changes in

233 both the maxilla and the dentition during growth. The morphological changes of the mandible  
234 have been frequently simplified by measuring only certain linear parameters, such as the  
235 mandibular length (distance between Condylion and Gnathion) (Mitani & Sato, 1992; Baccetti et  
236 al. 2005), bigonial breadth (the distance between two gonias) or bicondylar breadth (the straight  
237 distance between the most lateral points on the two condyles) (Vinay & Gowri, 2013). The  
238 orthodontic cephalometric literature has been preoccupied with the vertical and sagittal  
239 relationships, but the actual changes involve every region of the mandible and are composed of  
240 diverse three-dimensional growth vectors (Moyers & Bookstein, 1979). We confirm in three  
241 dimensions that the condyle shows active morphological changes, elongating predominantly  
242 posteriorly and superiorly along with the lengthening of the ramus. The mandibular body also  
243 elongates so as to permit the dental arc to accommodate more permanent teeth. The chin  
244 protrudes distinctively over time. These processes contribute to the known vertical and sagittal  
245 changes in the mandible. The changes in the transverse dimension are more subtle. It is  
246 well-established that the ossification of the mandibular symphysis occurs shortly after birth so  
247 after that time, changes in mandibular width would be expected to occur only by surface  
248 apposition or resorption. Nonetheless, in our analysis the left and right rami mandibular body  
249 diverge laterally, but by less than 4mm. These transverse changes may be constrained because  
250 the middle cranial fossa and its neural contents have stopped growing in early childhood and the  
251 bi-condylar width is fixed thereafter (Enlow & Hans, 2008).

252

253 We found sex differences in the overall size of the mandible. The mandibles of males are  
254 significantly larger than those of females over the whole of the study period. This trait has been  
255 documented by anthropologists and has been used for sex determination in forensic practice and  
256 for medico-legal purposes (Sikka & Jain, 2016; Sharma et al. 2016). Our study further shows how  
257 the size difference of the mandible between males and females gradually develops. At age 9, the  
258 mandibular size is generally larger in males than in females. The males and females show similar  
259 rates of change in size from 9 to 12 years. Thereafter the size increment slows down gradually in  
260 females but not in males until 17 years old. The overall greater mandibular size in males may  
261 relate to the greater masticatory forces to which the male mandible is subject. On average,  
262 females produce weaker muscle forces during mastication, resulting in smoother surfaces of

263 muscle attachments and smaller sized mandibles, whereas males have larger mandibles and  
264 produce stronger muscle forces (Vodanović et al. 2006; Velemínská et al. 2012).

265

266 Our study quantifies the annual change at a dense array of points over the mandible and  
267 visualizes the differential growth between males and females during adolescence. Growth in both  
268 male and female mandibles is rapid at the condyles and the chin, and to a lesser degree in the  
269 body of the ramus. Peak adolescent growth velocity is later in males than in females, which  
270 agrees with the finding in previous 2D studies (Nanda 1955; Buschang et al. 1989). It is the  
271 continuation of this growth pattern in males which results in the differences in form between  
272 male and female mandibles. This confirms that sexual dimorphism in the craniofacial structures is  
273 mainly the result of a differential growth rate after puberty and during adolescence (Ursi et al.  
274 1993; Rosas & Bastir 2002).

275

276 A strength of the current study is the sophisticated modelling technique. Some previous studies  
277 of soft and hard tissue growth from cross-sectional data use the first principal component (PC) as  
278 the growth trajectory (Hammond et al. 2004; Hammond et al. 2012; Suttie et al. 2013; Ibrahim et  
279 al. 2016). The first PC is the direction of greatest variability in the sample. Where the sample is of  
280 heterogeneous ages this often correlates strongly with age, but there is no guarantee that it is  
281 the dimension of variation that is most strongly correlated with age. Furthermore, it is limited in  
282 that it assumes growth proceeds along the same growth vectors throughout development (i.e.  
283 that growth is linear). On the contrary, the modeling approach used in this study allows growth  
284 vectors to change, depending on the age. Another strength is the use of color-maps to illustrate  
285 these growth vectors. This differs from the standard approach in geometric morphometrics,  
286 which is to plot growth patterns abstractly as lines in the subspace spanned by two or three  
287 principal components. In such a subspace inferences about differences between growth  
288 trajectories cannot really be made since the impression can change radically dependent on the  
289 choice of subspace (Mitteroecker et al. 2005).

290

291 The analysis of the morphological changes and the sex differences of the mandible has important  
292 implications for clinicians. When planning orthodontic treatment, the general intention is to

293 target the active growing sites and take advantage of accelerated or intense growth periods. Our  
294 study is consistent with previous findings that the greatest morphological changes during growth  
295 occur in the condyles (Nanda, 1955; Buschang et al., 1988) and therefore orthopedic forces  
296 should be applied to the condyles so as to encourage or restrict the mandibular growth (Hägg &  
297 Taranger 1982). (Deguchi et al. 2002). Our study also confirms the empirical practice of initiating  
298 orthodontic treatment earlier in females and delaying orthognathic surgery till after 16 years in  
299 females and after 18 in males when growth has plateaued (Weaver et al. 1998).

300

301 Determination of sex from an unknown human mandible is useful in forensic and anthropology  
302 field. Even though the mandible carries more information about a child's age than other bones,  
303 determining the gender of an isolated mandible remains a problem of shape. Franklin et al.  
304 suggests that it is difficult to use the subadult mandible for sex determination. It is not manifest  
305 at an appreciable level until after pubertal modifications have taken place (Franklin et al. 2007).  
306 Coquerelle et al. found that there is significant mandibular shape difference between males and  
307 females at birth. They found that this dimorphism diminishes so that there is no difference  
308 between male and female average shapes between age 4 of years and ~14 years. (Coquerelle et  
309 al. 2011). Our study is consistent with their findings of no statistically significant difference in the  
310 mandibular shape from 9 to 10 years of age, however, both of these findings should be treated  
311 cautiously since sample sizes at these ages were small in both studies. With a larger sample size,  
312 we have been able to identify a sex difference in shape by age 11. The dimorphic features extend  
313 and become more obvious during adolescence.

314

315 Our study further shows how the dimorphic features develop comprehensively in 3D. The chin is  
316 one of the most distinctive anatomical traits of modern humans. We found that adult males end  
317 up with more protruded, broader and almost square chins while adult females are characterized  
318 as narrower and more rounded. This agrees with the descriptions of Thayer et al. (Thayer &  
319 Dobson, 2010) and Coquerelle et al. (2011). The mandibular angle is more prominent in males  
320 than in females and this trait is preserved from pre-teen to post-teen. The mandibular angle is  
321 acted on by the masseter muscle, and differential biomechanical forces may explain this sex  
322 difference. It should be possible, using the data from this study to automate sex prediction from

323 an image of an isolated mandible using dense morphometric techniques.  
324  
325 The use of modern imaging technologies provides detail of bone anatomy without the need to  
326 dissect or compromise the integrity of skeletal material (Franklin et al. 2016). This is an especially  
327 valuable tool for investigating of the morphological changes in bone. Although growth related  
328 changes are ideally investigated longitudinally, to the best of our knowledge, only four studies  
329 have investigated longitudinal changes of the mandible in 3D. Three of these studies were limited  
330 by very small sample sizes (Bro-Nielsen et al. 1997; Andresen et al. 1998; Andresen et al. 2000).  
331 They also applied restrictive, biologically implausible mathematical forms to growth, assuming it  
332 follows either a linear or polynomial trajectory. Krarup et. al evaluated mandibular growth and  
333 tooth eruption on 10 children with Apert syndrome without commenting on mandibular form  
334 changes or sexual dimorphism (Krarup et al. 2005). Furthermore despite contemporary  
335 understanding that the mandible is unaffected in individuals with Apert Syndrome (Kreiborg et al.  
336 1999), it has yet to be ascertained that the syndromic group is characterized as the same growth  
337 trajectory as otherwise unaffected individuals. As there will always be difficulty obtaining  
338 sufficient numbers of longitudinal CBCTs of otherwise normal individuals due to ethical  
339 limitations, we used cross-sectional images collected prior to orthodontic treatment. We also  
340 applied a flexible, non-linear modelling technique that does not assume any particular form to  
341 the growth trajectory (Matthews et al. 2018). To the best of our knowledge, only Coquerelle et al.  
342 employed piecewise linear regressions to approximate a non-linear growth trajectory and to  
343 estimate expected mandibles from birth to 20 years of age (Coquerelle et al. 2011). This is  
344 conceptually quite similar to our method, however, they relied on projection of each growth  
345 trajectory into the subspace spanned by the first three principal components to investigate  
346 differences in rate of change and growth direction between the sexes which is limited for the  
347 reasons described earlier. A limitation of our study is that it evaluates the mandibular changes  
348 indexing by chronological age only. As there is considerable variation in the age at which children  
349 reach puberty, chronological age may not reflect developmental stage sufficiently and accurately,  
350 particularly for adolescents (Baccetti et al. 2005). Additional biological measurements, such as  
351 skeletal age or ossification stages, could potentially be added to the model in the future. Also,  
352 this is a clinical cohort which may include more orthodontic skeletal class II and III individuals

353 than the general population. A cohort of 'normal' individuals would be preferable for such a study,  
354 but CT/CBCT imaging of such a cohort would be difficult to justify.

355

### 356 **Conclusions**

357 Sexual dimorphism in the mandible results from the initial pre-teen difference and growth rate  
358 difference between males and females during pubertal growth trajectories. Mandibular sexual  
359 dimorphism already exists at nine years of age, but this is mostly in size not in shape. Growth  
360 direction in both males and females is similar but is faster, peaks later, and occurs over a longer  
361 period in males than in females. This results in increasing dimorphism in form which is evident in  
362 both size and shape. The dense morphometric approach provides detailed quantitative  
363 assessment in understanding the developmental mandibular sexual dimorphism in 3D.

364

### 365 **Acknowledgements**

366 We would like to thank Dr. Paul Buchholz for sharing the CBCT images used in this study.

367

### 368 **Conflict of Interest**

369 None

370

### 371 **Author contributions**

372 Y.F. contributed to the design of the work, performed all the analysis under the supervision of  
373 H.M. and wrote the first draft of the manuscript. H.M. implemented the kernel regression model  
374 and played an important role in interpreting the results. N.K., R.H. and A.P. contributed to  
375 constructive discussion and revised the manuscript critically for important intellectual content.  
376 P.S. and P.C. revised the manuscript. All authors have read and approved the final manuscript.  
377 Our dear colleague John Clement, who's vision was instrumental in initiating this body of work  
378 tragically died while the manuscript was in preparation. He is greatly missed.

379

380

### 381 **References**

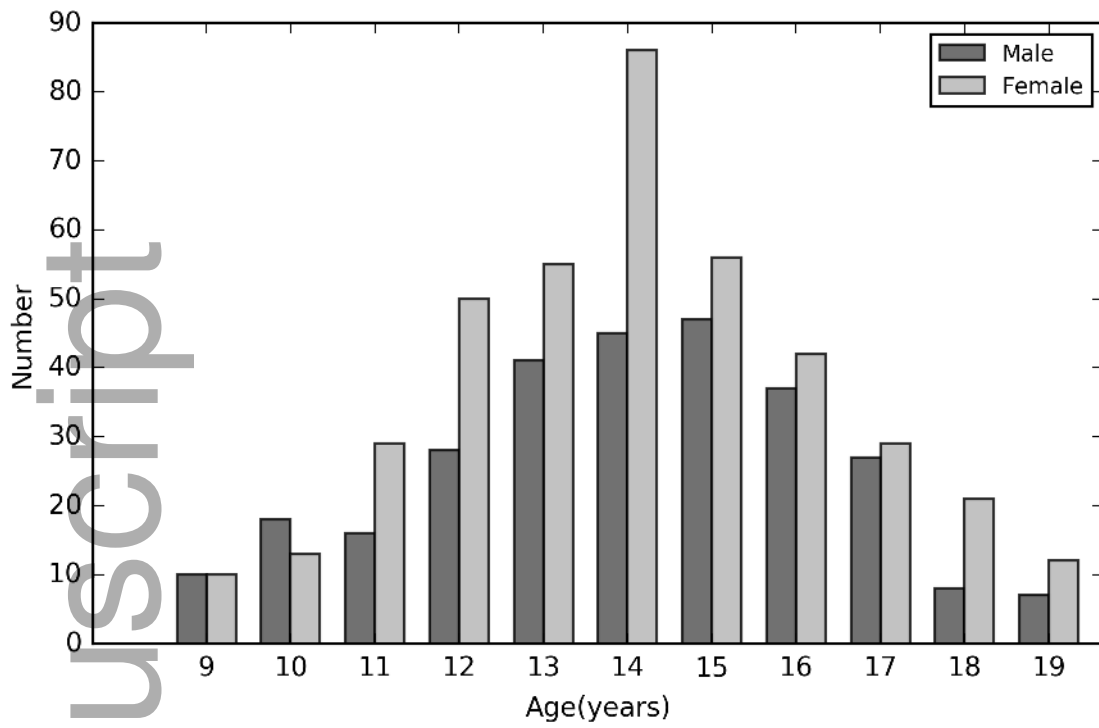
382 Andresen PR, Bookstein FL, Couradsen K, et al. (2000) Surface-bounded growth modeling applied to

- 383 human mandibles. *IEEE Transactions on Medical Imaging* **19**, 1053–1063.
- 384 Andresen PR, Nielsen M, Kreiborg S (1998) 4D shape-preserving modelling of bone growth. In
- 385 Proceedings of *Medical Image Computing and Computer-Assisted Intervention*, Springer, Berlin,
- 386 Heidelberg, 710–719.
- 387 Baccetti T, Franchi L, McNamara JA (2005) The cervical vertebral maturation (CVM) method for the
- 388 assessment of optimal treatment timing in dentofacial orthopedics. *Seminars in Orthodontics* **11**,
- 389 119–129.
- 390 Björk A (1968) The use of metallic implants in the study of facial growth in children: Method and
- 391 application. *American Journal of Physical Anthropology* **29**, 243–254.
- 392 Björk A (1963) Variations in the growth pattern of the human mandible: longitudinal radiographic
- 393 study by the implant method. *Journal of Dental Research* **42**, 400–411.
- 394 Brereton RG (2015) The Mahalanobis distance and its relationship to principal component scores.
- 395 *Journal of Chemometrics*, **29**, 143–145.
- 396 Bro-Nielsen M, Gramkow C, Kreiborg S (1997) Non-rigid image registration using bone growth model.
- 397 In *Proceedings of CVRMed-MRCAS*. 1–12.
- 398 Buschang PH, Tanguay R, Demirjian A, et al. (1989) Modeling longitudinal mandibular growth:
- 399 Percentiles for gnathion from 6 to 15 years of age in girls. *American Journal of Orthodontics and*
- 400 *Dentofacial Orthopedics*, **95**, 60–66.
- 401 Carlson DS (2005) Theories of craniofacial growth in the postgenomic era. *Seminars in Orthodontics*,
- 402 **11**, 172–183.
- 403 Claes P, Daniels K, Walters M, et al. (2012b) Dymorphometrics: the modelling of morphological
- 404 abnormalities. *Theoretical biology & medical modelling* **9**,5.
- 405 Claes P, Walters M, Clement J (2012a) Improved facial outcome assessment using a 3D
- 406 anthropometric mask. *International journal of oral and maxillofacial surgery* **41**, 324–30.
- 407 Coquerelle M, Bookstein FL, Braga J, et al. (2011) Sexual dimorphism of the human mandible and its
- 408 association with dental development. *American Journal of Physical Anthropology* **145**, 192–202.
- 409 Deguchi T, Kuroda T, Minoshima Y, et al. (2002) Craniofacial features of patients with Class III
- 410 abnormalities: Growth-related changes and effects of short-term and long-term chinup
- 411 therapy. *American Journal of Orthodontics and Dentofacial Orthopedics* **121**, 84–92.
- 412 Enlow DH, Hans MG (2008) *Essentials of facial growth*. Needham Press.

- 413 Enlow DH, Harris DB (1964) A study of the postnatal growth of the human mandible. *American Journal*  
414 *of Orthodontics* **50**, 25–50.
- 415 Fan Y, Beare R, Matthews H, et al. (2018) Marker-based watershed transform method for fully  
416 automatic mandibular segmentation from CBCT images. *Dentomaxillofacial Radiology*, **47**,  
417 20180261.
- 418 Franchi L, Baccetti T, McNamara JA (2001) Thin-plate spline analysis of mandibular growth. *The Angle*  
419 *orthodontist* **71**, 83–9.
- 420 Franklin D, Oxnard CE, O'Higgins P, et al. (2007) Sexual Dimorphism in the Subadult Mandible:  
421 Quantification Using Geometric Morphometrics. *Journal of Forensic Sciences*, **52**, 6–10.
- 422 Franklin D, Swift L, Flavel A (2016) "Virtual anthropology" and radiographic imaging in the Forensic  
423 Medical Sciences. *Egyptian Journal of Forensic Sciences* **6**, 31–43.
- 424
- 425 Hägg U, Taranger J (1982) Maturation indicators and the pubertal growth spurt. *American Journal of*  
426 *Orthodontics* **82**, 299–309.
- 427 Hammond P, Hutton TJ, Allanson JE, et al. (2004) 3D analysis of facial morphology. *American Journal*  
428 *of Medical Genetics*, **126A**, 339–348.
- 429 Hammond P, Hannes F, Suttie M, et al. (2012) Fine-grained facial phenotype–genotype analysis in  
430 Wolf–Hirschhorn syndrome. *European Journal of Human Genetics*, **20**, 33–40.
- 431 Hutton TJ, Buxton BF, Hammond P, et al. (2003) Estimating average growth trajectories in shape-space  
432 using kernel smoothing. *IEEE Transactions on Medical Imaging*, **22**, 747–753.
- 433 van der Haven I, Mulder JW, van der Wal KG, et al. (1997) The jaw index: new guide defining  
434 micrognathia in newborns. *The Cleft palate-craniofacial journal* **34**, 240–1.
- 435 Hu K-S, Koh K-S, Han S-H, et al. (2006) Sex determination using nonmetric characteristics of the  
436 mandible in Koreans. *Journal of Forensic Sciences* **51**, 1376–1382.
- 437 Ibrahim A, Suttie M, Bulstrode NW, et al. (2016) Combined soft and skeletal tissue modelling of normal  
438 and dysmorphic midface postnatal development. *Journal of Cranio-Maxillofacial Surgery*, **44**,  
439 1777–1785.
- 440 Kharoshah MAA, Almadani O, Ghaleb SS, et al. (2010) Sexual dimorphism of the mandible in a modern  
441 Egyptian population. *Journal of Forensic and Legal Medicine* **17**, 213–215.
- 442 Krarup S, Darvann TA, Larsen P, et al. (2005) Three-dimensional analysis of mandibular growth and

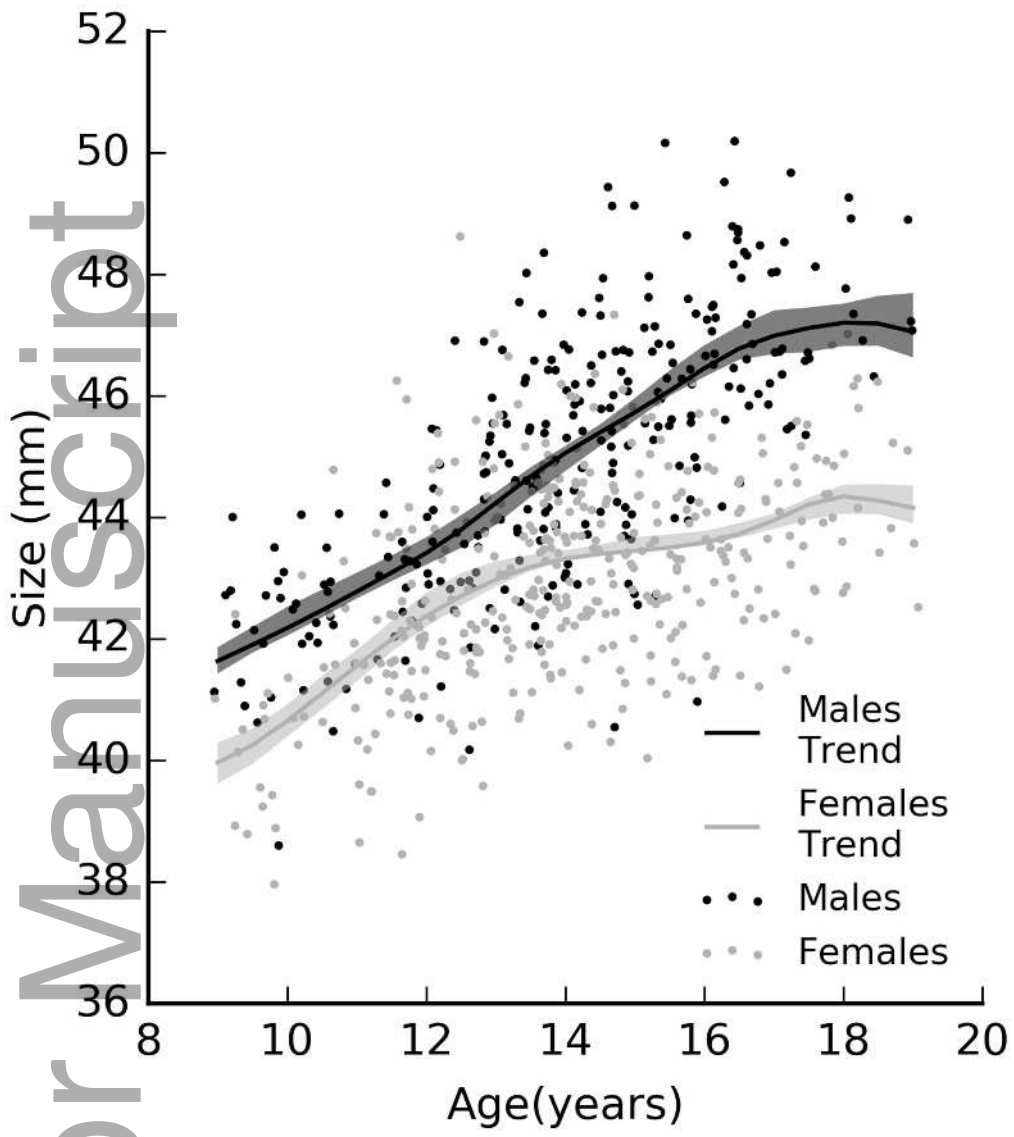
- 443 tooth eruption. *J Anat*, **207**, 669–682.
- 444 Kreiborg S, Aduss H, Cohen MM (1999) Cephalometric study of the Apert syndrome in adolescence  
445 and adulthood. *Journal of craniofacial genetics and developmental biology* **19**, 1–11.
- 446 Krstajic D, Buturovic LJ, Leahy DE, et al. (2014) Cross-validation pitfalls when selecting and assessing  
447 regression and classification models. *Journal of Cheminformatics*, **6**, 10.
- 448 Matthews HS (2018) Changing the face of craniofacial growth curves: Modelling growth and sexual  
449 dimorphism in children and adolescents using spatially dense 3D image analysis. The University  
450 of Melbourne.
- 451 Matthews HS, Penington AJ, Hardiman R, et al. (2018) Modelling 3D craniofacial growth trajectories  
452 for population comparison and classification illustrated using sex-differences. *Scientific Reports*  
453 **8**, 4771.
- 454 Mitani H & Sato K (1992) Comparison of mandibular growth with other variables during puberty. *The*  
455 *Angle orthodontist*, **62**, 217–22.
- 456 Mitteroecker P, Gunz P (2009) Advances in geometric morphometrics. *Evolutionary Biology* **36**,  
457 235–247.
- 458 Mitteroecker P, Gunz P & Bookstein FL, (2005) Heterochrony and geometric morphometrics: A  
459 comparison of cranial growth in *Pan paniscus* versus *Pan troglodytes*. *Evolution and*  
460 *Development*, **7**, 244–258.
- 461 Moyers RE, Bookstein FL (1979) The inappropriateness of conventional cephalometrics. *American*  
462 *Journal of Orthodontics* **75**, 599–617.
- 463 Nanda RS (1955) The rates of growth of several facial components measured from serial  
464 cephalometric roentgenograms. *American Journal of Orthodontics*, **41**, 658–673.
- 465 Nadaraya ÉA (1965) On Non-Parametric Estimates of Density Functions and Regression Curves. *Theory*  
466 *of Probability & Its Applications*, **10**, 186–190.
- 467 Popa MF, Stefanescu CL, Corici PD (2009) Forensic value of mandibular anthropometry in gender and  
468 age estimation. *Romanian Journal of Legal Medicine* **17**, 45–50.
- 469 Rosas A & Bastir M (2002) Thin-plate spline analysis of allometry and sexual dimorphism in the human  
470 craniofacial complex. *American journal of physical anthropology*, **117**, 236–45.
- 471 Sharma M, Gorea RK, Gorea A, et al. (2016) A morphometric study of the human mandible in the  
472 Indian population for sex determination. *Egyptian Journal of Forensic Sciences* **6**, 165–169.

- 473 Sikka A, Jain A (2016) Sex determination of mandible: a morphological and morphometric analysis.  
474 *International Journal of Contemporary Medical Research* **3**, 1869–1872.
- 475 Suttie M, Foroud T, Wetherill L, et al. (2013) Facial Dysmorphism Across the Fetal Alcohol Spectrum.  
476 *Pediatrics*, **131**,e779–e788.
- 477 Thayer ZM, Dobson SD (2010) Sexual dimorphism in chin shape: Implications for adaptive hypotheses.  
478 *American Journal of Physical Anthropology* **143**, 417–425.
- 479 Ursi WJ, Trotman CA, McNamara Jr JA, et al. (1993) Sexual dimorphism in normal craniofacial growth.  
480 *The Angle Orthodontist*, **63**,47–56.
- 481 Velemínská J, Bigoni L, Krajíček V, et al. (2012) Surface facial modelling and allometry in relation to  
482 sexual dimorphism. *HOMO*, **63**, 81–93.
- 483 Vinay G, Gowri M (2013) Sex determination of human mandible using metrical parameters. *Journal of*  
484 *clinical and diagnostic research* **7**, 2671–3.
- 485 Vodanović M, Dumančić J, Demo Ž, et al.(2006) Determination of sex by discriminant function analysis  
486 of mandibles from two Croatian archaeological sites. *Acta stomatologica Croatica*, **40**, 679–89.
- 487 Watson GS (1964). Smooth regression analysis. *Sankhyā: The Indian Journal of Statistics, Series A*,  
488 359–372.
- 489 Weaver N, Glover K, Major P, et al. (1998) Age limitation on provision of orthopedic therapy and  
490 orthognathic surgery. *American journal of orthodontics and dentofacial orthopedics*  
491 **113**,156–64.
- 492 Wei R, Claes P, Walters M, et al. (2011) Augmentation of linear facial anthropometrics through  
493 modern morphometrics: a facial convexity example. *Australian Dental Journal* **56**, 141–147.

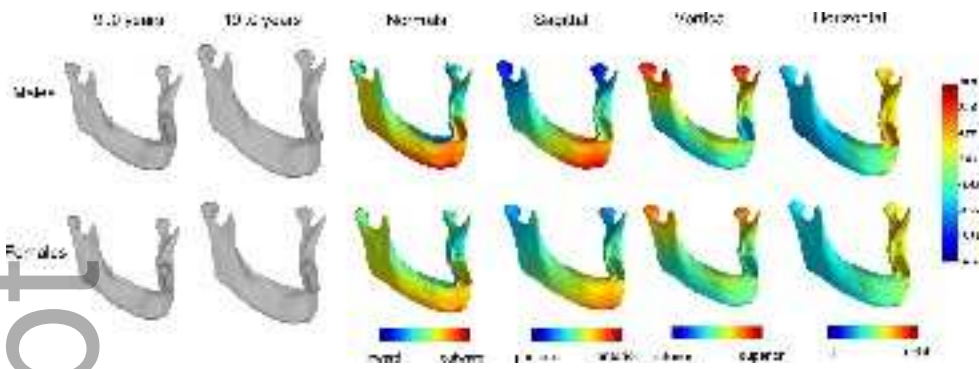


joa\_12949\_f1.tiff

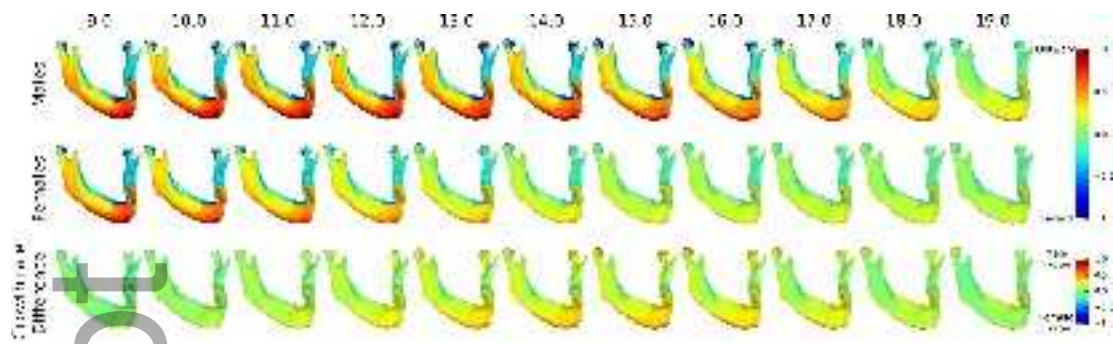
Author Manuscript



joa\_12949\_f2.tif

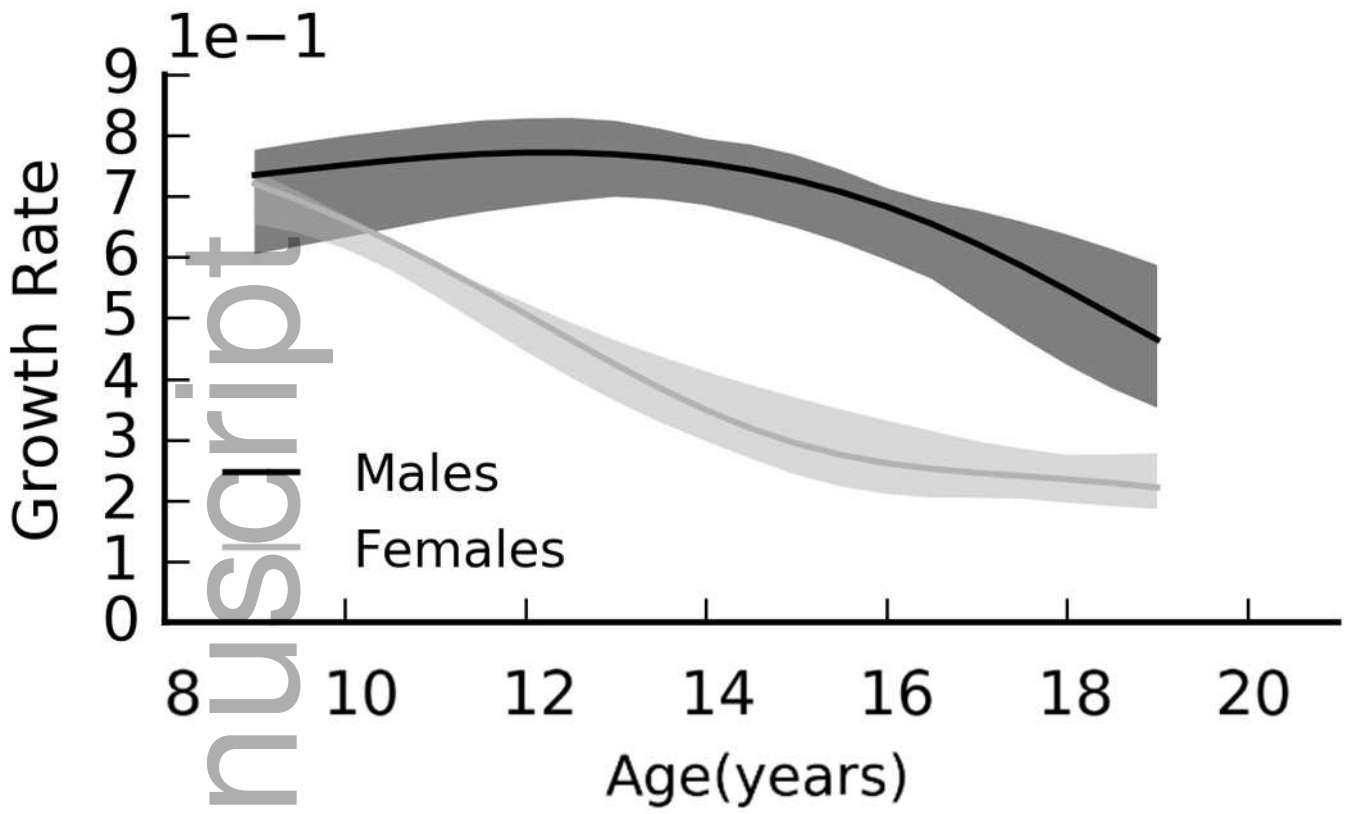


joa\_12949\_f3.tif



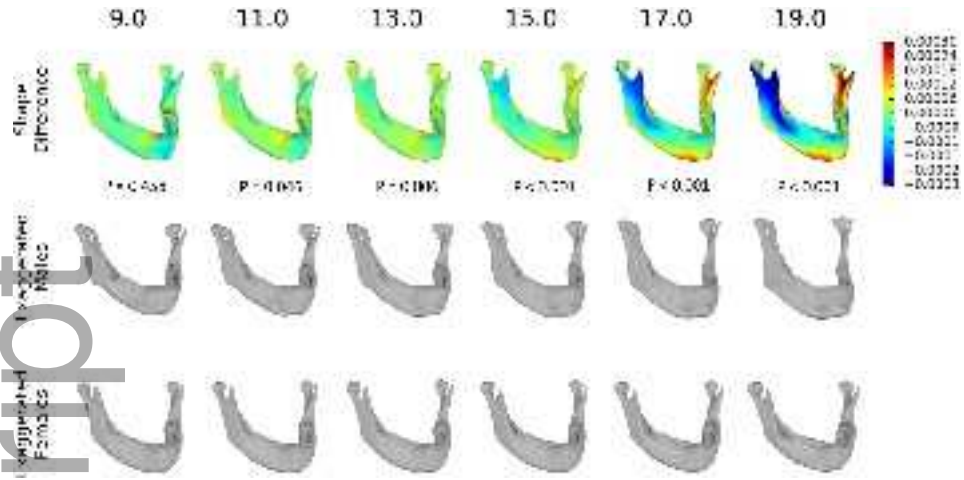
joa\_12949\_f4.tiff

Author Manuscript



joa\_12949\_f5.tif

Author Manuscript



joa\_12949\_f6.tif